Title
EEG Microstates in Neurofeedback Attention Training

Permalink
https://escholarship.org/uc/item/8cp0339j

Author
Sipes, Benjamin Snow

Publication Date
2019

Peer reviewed|Thesis/dissertation

EEG Microstates in Neurofeedback Attention Training

by
Benjamin Sipes

THESIS
Submitted in partial satisfaction of the requirements for degree of
MASTER OF SCIENCE

in

Biomedical Imaging

in the

GRADUATE DIVISION
of the
UNIVERSITY OF CALIFORNIA, SAN FRANCISCO

Approved:

DocuSigned by:
Srikantan Nagarajan   Srikantan Nagarajan
4C21BC1B9EB145E...
                                                                    Chair

DocuSigned by:
Adam Gazzaley   Adam Gazzaley
DocuSigned by:54D6...
Valentina Pedoia   Valentina Pedoia
DocuSigned by:842C...
Alastair Martin   Alastair Martin
0D642C3C2048404...

Committee Members

Acknowledgements

EEG Microstates in Neurofeedback Attention Training

Benjamin Sipes

Abstract

Attention has come under acute focus within the neuropsychological world in past decades, and the rise of brain-computer interfaces (BCI) during EEG offers a means to personalize attention training therapies. Semi-stable EEG topographies, called "microstates," have been found to be functionally relevant to attention-oriented tasks and shown to influence awareness in the time period directly before a stimulus. In a BCI designed to train attention, we may expect to see a group difference in microstates. Specifically, it could be that microstate D—functionally relevant to attention and task-switching—increases while microstate C—functionally relevant to task-negative and saliency networks—decreases within the group that successfully learns via neurofeedback. The reversed pattern may be true in groups that either fails to learn through neurofeedback or received sham neurofeedback. We may also expect microstates D and C to relate to a behavioral outcome measure that indexes training performance. Accordingly, we used EEGLAB to process BCI attention-training data, derive microstate topographies for individual participants, cluster grand mean topographies for the entire study group, and extract temporal statistics to measure microstate temporal presence during pre-stimulus training. Overall, microstate D had greater temporal presence in those who successfully self-regulated neural cognition during the BCI task compared to those who could not achieve this; microstate C had greater temporal presence in those who could not self-regulate neural cognition during the BCI task compared to those who did so successfully. This analysis highlights differences in BCI performance, but failed to find meaningful changes over training.

Table of Contents

List of Figures

List of Tables

1. Introduction

Attention has come under acute focus within the neuropsychological world in past decades. With the so-called Attention-deficit/hyperactivity disorder (ADHD) "epidemic," much research is invested to better understand the executive systems in the brain that modulate attention and influence its deficits. Likewise, stakeholders heavily invest in ways to improve attention. Drugs such as Adderall and Ritalin are marketed as panaceas to this epidemic, yet their value, efficacy, and ethics within their target population—young adults with ADHD—are actively debated. However, pharmacological substances are not the only means we may deploy to influence neurobiology. Games and training programs also show efficacy as therapeutic treatments for cognitive deficits (Anguera et al., 2013). Furthermore, the rise of BCI during EEG offers a means to personalize training paradigms such that they give real-time neurofeedback, thus enhancing the learning experience (Curran & Stokes, 2003). Many BCIs deploy source localization algorithms to index their feedback. However, this strategy may be a limitation. Many brain regions participate simultaneously in complex cognitive tasks, and source localizing is challenging due to EEG's ill-posed inverse problem. There may be other EEG derived signatures that better index complex cognitive performance.

EEG microstates are semi-stable patterns of electric-field surface potential topographies. They form characteristic and reproducible polarity maps that can be extracted from a full EEG timeseries and utilized to query functional neurobiological systems (Wakermann et al., 1992; Khanna, Pascual-Leone, & Farzan, 2014). Microstate analyses capture inherent features of cortical connectivity patterns that are representative of well-defined networks identified through other imaging modalities—namely fMRI—and thought to be subdivisions of the characteristic default mode network (DMN) (Bréchet et al., 2019; Britz, Van De Ville, & Michel, 2010;

Pascual-Marqui et al., 2014; Seitzman et al., 2017). Unlike fMRI, they exploit EEG's excellent temporal resolution such that they observe connectivity moments at the sub-second scale with each microstate lasting between 50-120 milliseconds. Microstates are best measured through their temporal dynamics (Van De Ville, Britz, & Michel, 2010): microstate duration (average time active) and occurrence (times active per second). Their overall temporal presence as measured by dwell time, the product of duration and occurrence, offers an index for meaningful cognition. Microstate functional significance is under active investigation, but patterns are beginning to emerge regarding the significance of two commonly derived microstates classified in the literature as "C" and "D" (Michel & Koenig, 2018).

Among the first works attempting to derive functional significance in microstates, Britz and colleagues (2010) found that microstate C overlapped with cortical regions involved in the saliency network, and they speculated it to be involved in task-negative or task-ready mentation. In the same work microstate D overlapped with cortical regions involved in the ventral fronto-parietal areas related to attention networks. Milz and colleagues (2016) expanded on this work, finding that microstate D was especially focused in the posterior and anterior cingulate, positing that it had a role in attention-oriented activity and focus-switching. Seitzman and colleagues (2017) found microstate D temporal dynamics increased specifically during serial sevens subtraction while microstate C temporal dynamics decreased in this task, suggesting their task-positive/task-negative relationship. While these studies were contextualized in math and visualization tasks, Morris and colleagues (2018) additionally found that microstate D was active during audio-based attention also, suggesting more universality with its role in attention-oriented mentation. Most recently, Bréchet and colleagues (2019) found microstate C most active within a memory-retrieval task and activated areas overlapping with parietal networks also involved in

memory-retrieval. In the same work, they identified microstate D as most active during their math condition, overlapping with fronto-parietal control networks. Taken together, we may infer that microstate C generally relates to saliency networks, though its role as explicitly "task-negative" is debated. We may also infer that microstate D is involved in attention, though its exact role is still under investigation.

Furthermore, there is evidence to support microstates within a BCI context. Hernandez and colleagues (2016) found that microstate D was capable of modulation through neurofeedback and may be applicable to training in clinical populations. Additionally, Brtiz and colleagues (2014) found microstates to significantly modulate awareness when measured immediately pre-stimulus. Although the present study does not index neurofeedback through microstates, it may be helpful to analyze them in this attention BCI context.

In a BCI training attention, we may expect to see a group difference in microstates. Specifically, it could be that microstate D increases and microstate C decreases within the group that receives genuine neurofeedback, and the reversed pattern in a group that receives sham neurofeedback. We may also expect microstates D and C to relate to a behavioral outcome measure that indexes training performance. To test these hypotheses, we used EEG data collected from an attention training BCI paradigm. The experiment was structured such that there were two main healthy adult groups: one that received genuine neurofeedback training and another that received training with sham neurofeedback from an age and gender matched participant. Accordingly, we used MATLAB and the toolbox EEGLAB to conduct a microstate analysis (The MathWorks, Inc., Natick, Massachusetts, United States; Delorme & Makeig, 2004). Ultimately, we sought to determine if there were group differences in microstate temporal presence over the training period.

2. Methods

Participants

The cognitive Brain-Computer Interface (cBCI) project recruited 48 healthy adult participants (mean age 26 years, STD 2.4 years; 34 females). Recruitment sought to establish a 2:1 ratio between the experimental group and the control (sham) group. All participants were screened for non-ADHD status on the Adult ADHD Self-report Scale (ARSR-v1.1). Participants provided written informed consent for the study, and received payment in compensation for their participation.

Data Acquisition

Training data was acquired between October 2015 and October 2017. Each learning session lasted 40 minutes, during which 64-channel EEG was recorded and a closed loop neurofeedback provided performance information on a personalized scale. The scale was determined by the mean and variance of participants performance during an initial diagnostic assessment. The task adaptively modified challenge to match performance ability within each learning session. All learning sessions occurred over a mean of 31.8 days (SD = 19.7 days).

Learning consisted of a pattern/shape recognition and sustained attention task. There were ten experimental runs with 75 trials in each. At the beginning of every experimental run, participants were shown a target shape (either square, circle, diamond, pentagon, or hexagon— all equal areas) inside which had a grating at either 45 or 135 degrees. Within the task, participants received an audiovisual cue followed by a one-second delay, after which a visual target/non-target appeared. Target to non-target ratio was approximately 1:2. Participants had a brief and adaptive time to respond based on prior trials, and they responded using bumpers on a

platform controller. Response threshold equalized during the diagnostic assessment once participants reached 80% accuracy. Participants did not receive neurofeedback during the initial diagnostic session; however, they did receive neurofeedback during ten following training sessions on a 0-100-point scale—0 and 100 represent ±2.5 STD neural performance based on frontal-visual alpha coherence. This coherence is a measure of neural synchrony between left prefrontal and left extrastriate visual cortex where high coherence indicates mind-wandering and low coherence indicates attention. Coherence measures were acquired during the 500ms prior to target/non-target stimulus presentation. Challenge between trials was adaptive, with greater success rendering increased challenge where non-target stimuli are more visually alike to the target. Each training day's initial adaptive parameters are adjusted based on past training days. Participants receiving sham feedback were not given personalized neural metrics. Instead, their feedback mimicked those of age- and gender-matched experimental participants.

A behavioral outcome measure, efficiency, was determined for each session. As the task was adaptive, accuracy alone is not enough to index performance. Ideal performance in the task involves both speed and accuracy. Reaction time for each trial was recorded, and efficiency for each trial was defined as accuracy divided by reaction time. Efficiency measures over the entire training session were averaged into a mean efficiency for that session. This mean efficiency became the behavioral outcome measure to assess performance and compare neural data.

Training data included in the analysis came from either sessions 1 or 2—constituting the early training period—sessions 5 or 6—constituting the middle training period—and sessions 9 or 10—constituting the latest training period (**Figure 2.1**). These sessions were selected to observe outcome measures over the course of the 10-session training schedule. All six data time points for all participants entered preprocessing.
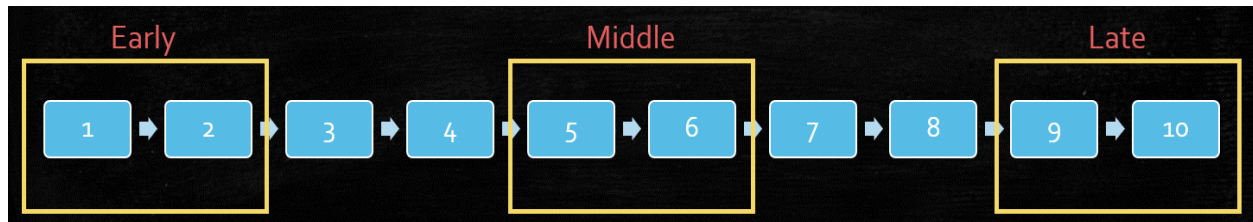

Figure 2.1: Diagram of the training schedule for all participants and the time-points drawn from it.

Preprocessing

We converted the raw files before preprocessing. The raw files were acquired using LSL in XDF format designed for BCIs. We used MATLAB 2016b and BCILAB functions to extract the raw files and save them as an EEGLAB EEG struct with channel locations rewritten to the 10-20 scheme used in the experiment. We ran preprocessing using a MATLAB plugin Automagic (Pedroni, Bahreini, & Langer, 2018). Automagic is an EEG preprocessing software that combines many of the leading processing algorithms to establish a comparable preprocessing standard.

Through Automagic, we used the PREP pipeline, which removes line noise and iteratively detects and interpolates bad channels (Bigdely-Shamlo, 2015). We also used the Multiple Artifact Rejection Algorithm (MARA), which performs independent component analysis across all channels to automatically detect and remove characteristic EEG artifacts (Winkler, Haufe, & Tangermann, 2011). The data was high-pass filtered at 1 Hz and low-pass filtered at 30 Hz.

Automagic provided a quality assessment that graded the data quality according to multiple measures. Automagic computed the ratio of bad channels (RBC) and the ratio of channels of high variance (CHV) per data session with default thresholds defining cutoffs for data quality assignment. These thresholds were as follows: Good < 0.15 < Ok < 0.3 < Bad. Automagic quality assessment also reports metrics for overall high amplitude (OHA) and time points of high variance (THV). These also had default thresholds as follows: Good < 0.1 < Ok < 0.2 < Bad. The final rating is a combination of all quality assessment ratings. (**Figure 2.2**)
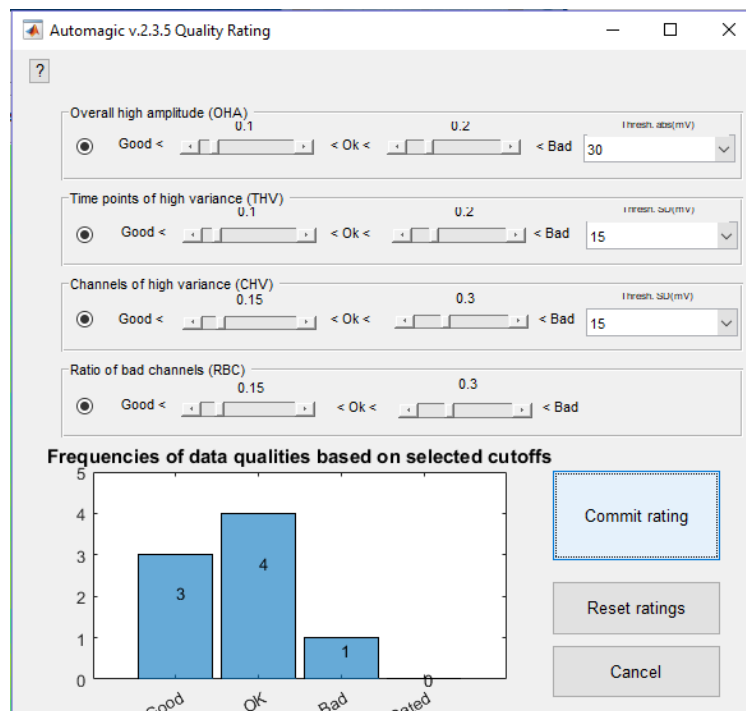

Figure 2.2: Automagic quality rating thresholds and data-quality visualization.

Quality rating for all data was made based on these default thresholds. Participants with "Bad" data from both sessions within the same time period (early, middle or late) were excluded from further analysis. A total of 11 participants were excluded in this manner (7 from the experimental group, and 4 from the sham group).

The remaining 37 participants had all their data proceed to the microstate analysis.

Microstate Analysis

EEGLAB processed the data and prepared it for microstate analysis. First, the data was down sampled to 256 Hz. Using the event information within the EEG struct, data were bounded to include 500 milliseconds at the end of the audiovisual cue—immediately prior to the target/non-target stimulus for each trial. This window was selected because it is the same window used within the training to measure the coherence provided in the neurofeedback.

The Microstate Analysis plugin for EEGLAB extracted microstates and calculated their temporal dynamics (Poulsen et al., 2018). Modified k-means clustering clusters EEG topographic information at global field power peaks in the EEG timeseries while ignoring polarity. K-means clustered EEG data for each participant and session individually. K-mean's convergence metric was cross-validation, and it chose the best solution over 10 initializations. The algorithm derived 4, 5, and 6 microstate clusters, and it was subsequently determined that 5 states offered the optimal cross validation metric and highest quality states. Two participants (both in the experimental group) had microstates across multiple time points that presented eyeblink artifacts, and were subsequently removed from further analysis.

Before group-level analysis, one session from each time point (early, middle, and late) was selected such that each participant had only a single training session's data per time point. This selection was determined by a random number generator and was subsequently checked for nonsignificant group differences between session-selection, gender, and age. (**Table 2.1**)

Table 2.1: Demographic information for all participants used in the final analysis. Experimental group divided into "Learners" and "Non-Learners." Statistics for Age and Gender are from an ANOVA analyzing the effect of group on Age and Gender. The final row compares the time points randomly selected per group. Statistics for Time Point Used uses t-tests to determine significance between groups.

Demographics/	Learners (L)	Non-Learners (NL)	Sham	Statistics
Gender	F = 8 M = 5	F = 8 M = 3	F = 9 M = 3	P = 0.82
Age	Mean = 26.15 yrs. STD = 2.04 yrs.	Mean = 26.18 yrs. STD = 2.79 yrs.	Mean = 25.0 yrs. STD = 3.41 yrs.	P = 0.39
Time Point Used	T1 = 7 T2 = 6 T5 = 5 T6 = 8 T9 = 5 T10 = 7	T1 = 4 T2 = 5 T5 = 5 T6 = 3 T9 = 4 T10 = 3	T1 = 6 T2 = 6 T5 = 6 T6 = 6 T9 = 7 T10 = 5	L vs NL P = 0.79 L vs Sham P = 0.52 NL vs Sham P = 0.40

All individual microstate topographic maps entered second-level group analysis. All maps were clustered again using k-means clustering algorithm with a correlation-based distance measure. There were 6 classes assigned in this second-level analysis. 6 classes were chosen to enhance comparability to a recently published work investigating microstate classes during a task (Bréchet et al., 2019). The algorithm provided a class assignment to each individual topographic map, and a grand mean template of each class assignment was generated. As no individual session could have two of the same microstates, ties in the second-level k-means clustering were broken as determined by a parametric correlation with the grand mean topographies. The

topographic map with the highest correlation with the grand mean class 'won' that class assignment. If there was another class correlation (rho > 0.8) in the 'losing' topography that was not yet an assigned microstate class expressed in that session, that became the new class assignment. Otherwise, the topography was excluded from the analysis—37 out of 510 (7.3%) of topographic map assignments became a null-assignment state and were subsequently excluded.

Following the microstate class assignment, the states were back-fit to the EEG data and smoothed the microstate labels by rejecting small segments. All microstates lasting for less than 30ms were temporally smoothed into microstate labels on either side of the small segment. As modified k-means clustering does not account for polarity, neither did the back-fitting algorithm. After the microstates were back-fit to the data, microstate statistics were calculated automatically by the toolbox and saved. These statistics included occurrence and duration for each microstate.

Statistical Analysis

From the microstate statistics output, the dwell time measure was derived by multiplying each session's respective duration and occurrence. Dwell time was used as a measure of temporal presence to compare microstates to each other. In the following analysis, we evaluate statistics for microstate C and microstate D due to their relevance to attention-oriented tasks.

Post-hoc analysis additionally revealed that a subset of the experimental group could not effectively self-regulate their neural coherence. Some experimental participants observed a negative coherence slope with sequentially successful trials (i.e. successful self-regulation), while other experimental participants observed a positive coherence slope with sequentially successful trials (i.e. unsuccessful self-regulation) (**Figure 2.3**). This difference in slope constituted the rational and definition to subdivide the experimental group into those participants
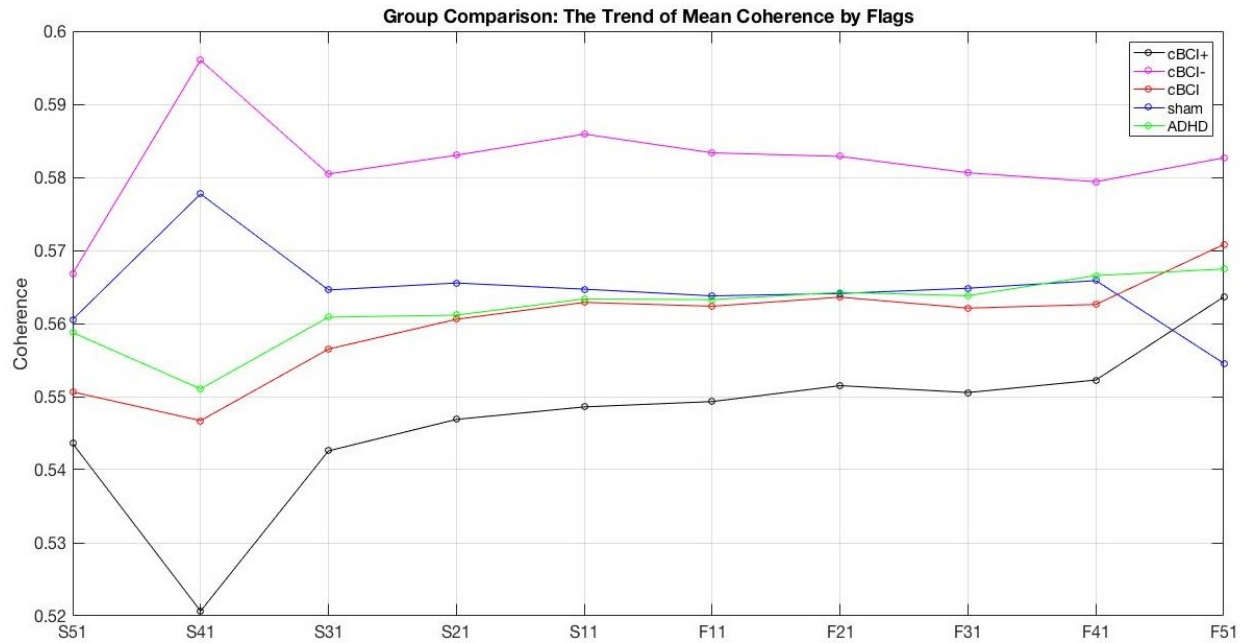
Figure 2.3: This is a graph of coherence measures over the course of training. S11 signifies having answered a trail correctly, and successive labels (S21, S31,…) signify multiple correct trials in a row. The opposite is true for F11 which signifies a single incorrect trial and subsequent incorrect trials in a row. The top-most line-plot depicts coherence in the group constituting the "Non-Learners," defined by their overall positive slope in coherence. The lower-most line-plot depicts coherence in the group constituting the "Learners," defined by their overall negative slope in coherence with increasing correct trials.

that could effectively self-regulate their coherence (Learners) and those participants that could not effectively self-regulate their coherence (Non-Learners). The 22 experimental participants whose data made it to the final analysis thus divided into 13 Learners and 9 Non-Learners.

ANOVA was evaluated to establish interactions in dwell time between group assignment, time-point, efficiency measure, and microstate. Following significant interactions, we performed two-sample t-tests to evaluate hypotheses. Non-parametric correlations additionally assessed interactions between the continuous measure, efficiency, and microstate dwell time. Lastly, we sought to examine the ratio of microstate C to microstate D to observe group effects of relative temporal presence when comparing the two microstates.

3. Results

Microstates Found

Five microstates were extracted for each participant and session individually. The five microstates per session on average had a total global explained variance of 70.4% (STD = 3.9%). Six microstates were clustered at the group level (**Figure 3.1**). This number does not optimize a specific criterion,
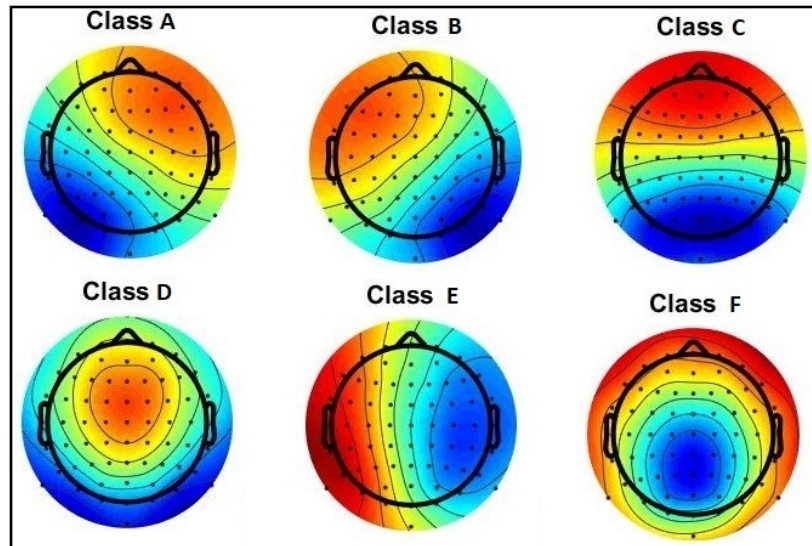

Figure 3.1: This is an image of the six grand mean topographies clustered at the group-level analysis. The statistics extracted for further analysis come from class C (upper right) and class D (lower left).

but instead replicates the number and form of states derived from Bréchet and colleagues (2019) as they analyze states during a memory/math task. The following statistic measures focused on only two of the six derived states (C and D).

ANOVA

Overall, the ANOVA revealed significant interactions with microstate C and D dwell times. Specifically, there was a significant microstate by group interaction, both when including the Sham group (p = 0.0002), and when excluding the Sham group (p < 0.0001). There was a trending microstate by efficiency interaction only when excluding the Sham group (p = 0.051). The ANOVA did not reveal significant changes over time based on group identity, both including the Sham group (p = 0.84) and excluding the Sham group (p = 0.68). Accordingly, the

following results collapse across all time points—they display the differences at a group level instead of change over the training period.

Dwell Time: Group vs Microstate

The literature relates microstate C with task-negative mentation. Microstate C dwell time in the Non-Learners group (mean = 258.72ms; STD = 21.89ms) was greater than the Learners (mean = 233.77ms; STD = 28.57ms) and that difference was significant (p = 0.0011). Non-Learners also had higher dwell time compared to and the Sham group (mean = 243.18ms; STD = 22.42ms) and that difference was significant (p = 0.015). The Learners compared to the Sham group showed no significant difference in microstate C dwell time between them (p = 0.14). Thus, during training, Non-Learners appear to have a significantly greater temporal presence of microstate C compared to both other groups. (**Figure 3.2a**)
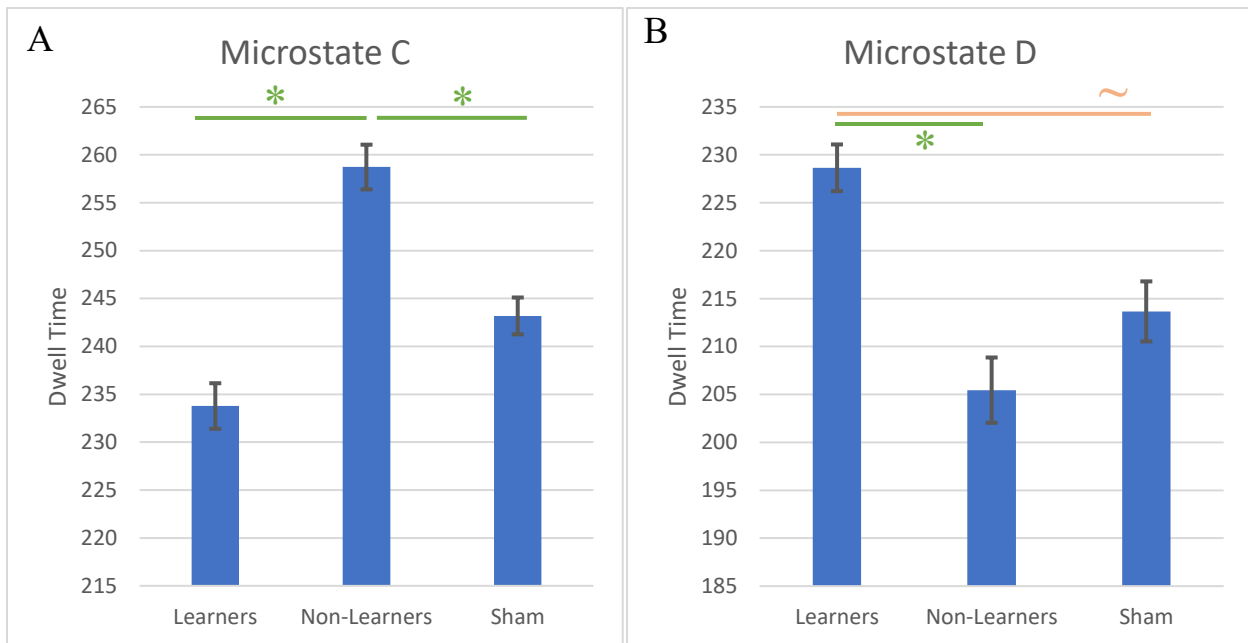

Figure 3.2: This depicts a bar-plot of microstate C (a) and microstate D (b) dwell times comparing between groups and collapsed across time.

The literature relates microstate D with attention-oriented mentation. Microstate D dwell time in the Learners group (mean = 228.64ms; STD = 29.6ms) was greater than the Non-Learners group (mean = 205.45ms; STD = 32.67ms) and that difference was significant (p = 0.0075). Learners also were greater than the Sham group (mean = 213.66ms; STD = 37.04ms), however this difference did not meet the threshold for significance (p = 0.069). Additionally, the Sham group was not significantly different compared to the Non-Learners in this microstate (p = 0.40). Thus, during training, Learners appear to have a significantly greater temporal presence of microstate D compared to both other groups. (**Figure 3.2b**)
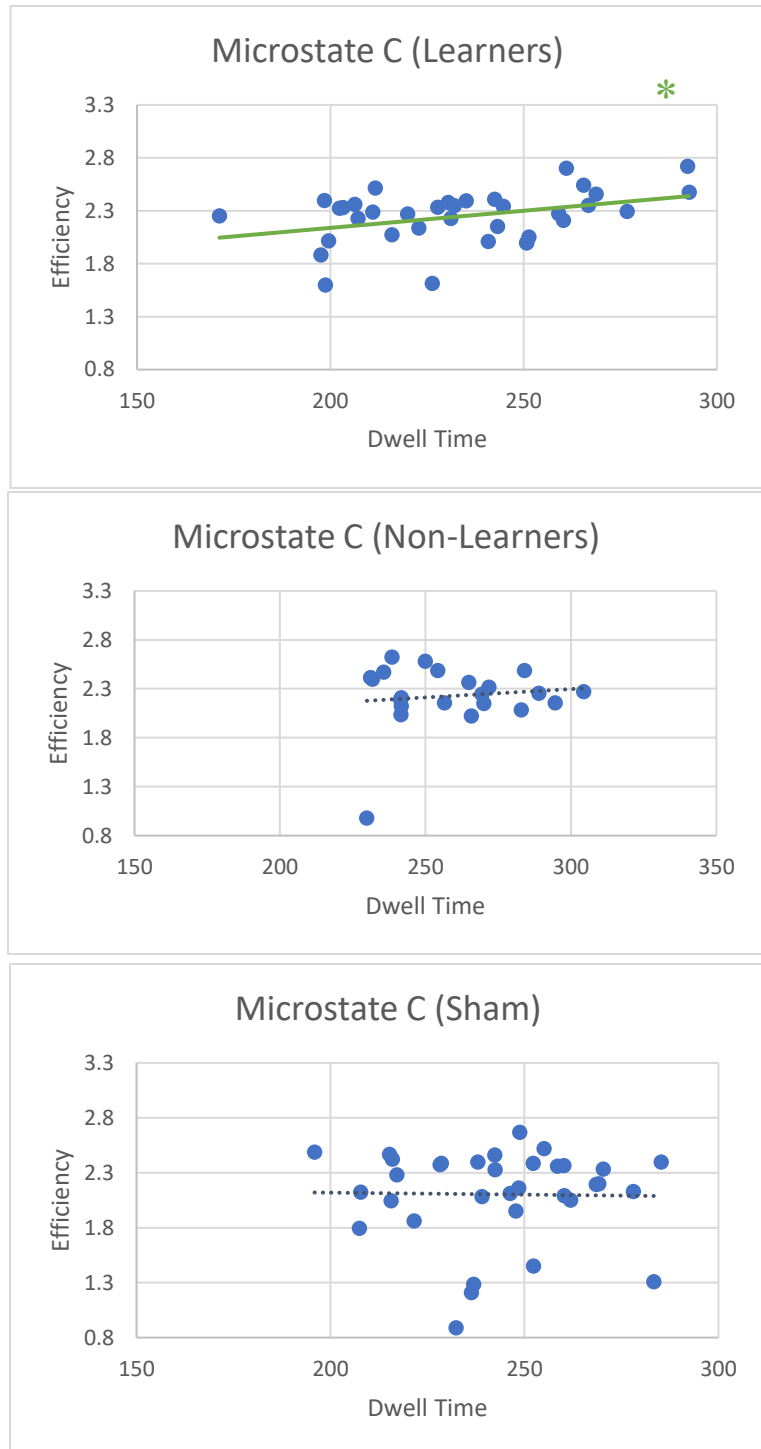

Figure 3.3: These are three scatter plots comparing microstate C dwell time to efficiency collapsed over all time points. Only the correlation in the Learners is significant.

Dwell Time: Group vs Efficiency

Microstate C dwell time was also compared to the continuous behavioral measure efficiency through a non-parametric Spearman's correlation. Learners had a significant *positive* relationship between microstate C and efficiency (rho = 0.35; p = 0.036). The Non-Learners group had no significant relationship with efficiency (rho = -0.09; p = 0.68). The Sham group had no significant relationship with efficiency (rho = 0.0023; p = 0.99). Thus, during training, microstate C dwell time has a group-based positive relationship with efficiency in Learners. (**Figure 3.3**)

Microstate D dwell time was also compared to the continuous behavioral measure efficiency through a non-parametric Spearman's correlation. Learners had a trending *negative* relationship between microstate

Figure 3.4: These are three scatter plots comparing microstate D dwell time to efficiency collapsed over all time points.

D and efficiency (rho = -0.32; p = 0.059). The Non-Learners group had no significant relationship with efficiency (rho = -0.005; p = 0.98). The Sham group also had no significant relationship with
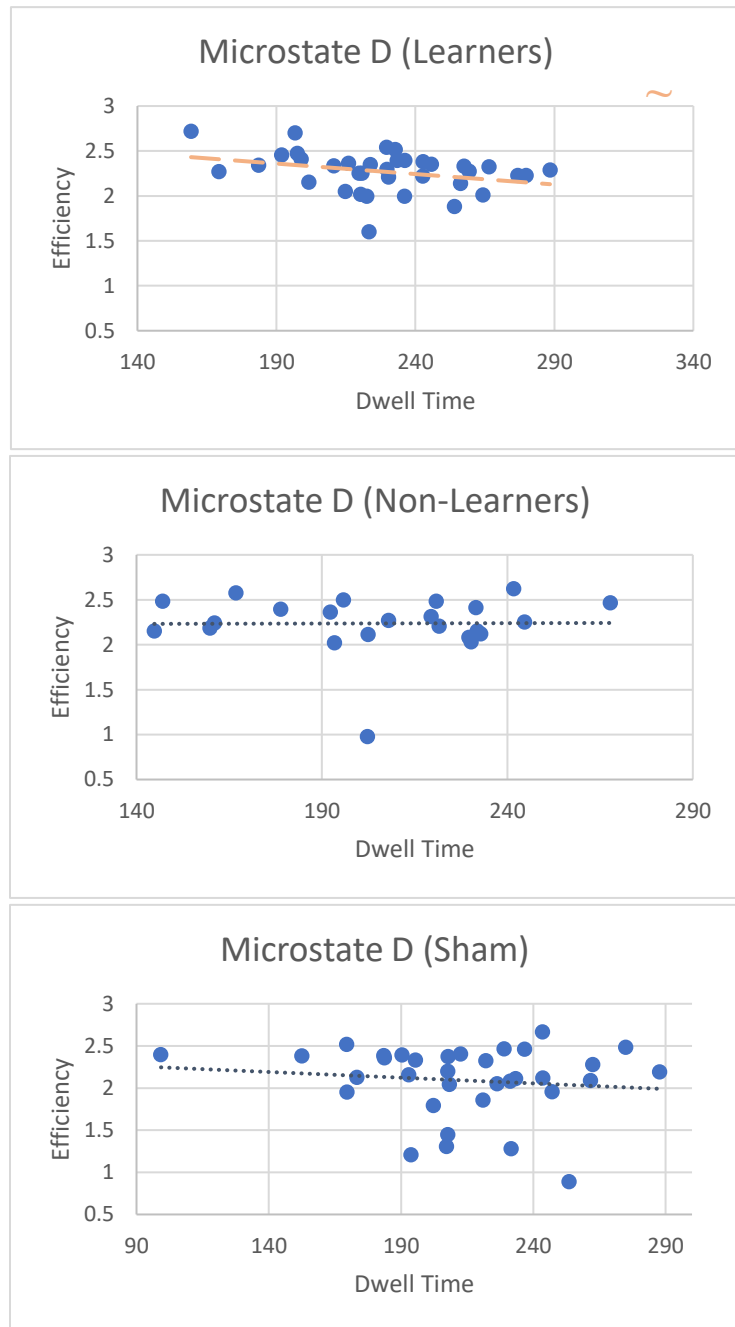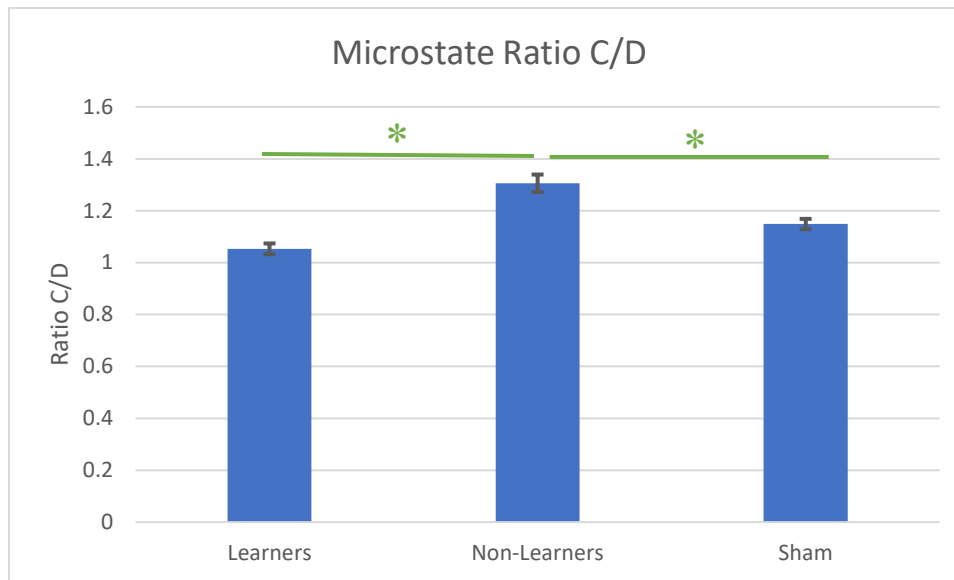
Figure 3.5: This depicts a bar-plot of microstate C dwell time divided by microstate D dwell time comparing between groups and collapsed across time. Learners compared to Non-Learners are significant, and Non-Learners compared to Sham are significant. Learners compared to Sham was non-significant.

efficiency (rho = -0.11; p = 0.55). Thus, during training, microstate D dwell time may have a group-based negative relationship with efficiency in Learners. (**Figure 3.4**)

Ratio of Microstate C to Microstate D

To investigate the balance in the temporal dependencies for microstates C and D, we divided same-session dwell times for microstate C by microstate D such that a value above 1 indicates higher temporal presence of microstate C, and a value below one indicates a higher temporal presence of microstate D. Learners were significantly more balanced in microstate C and D temporal presence (mean = 1.05; STD = 0.24) compared to Non-Learners (mean = 1.31; STD = 0.30), and this difference was significant (p = 0.0017). Sham participants displayed a ratio intermediate to the other groups (mean = 1.15; STD = 0.22), and was only significantly different from the Non-Learners (p = 0.041) with no significant difference compared to Learners (p = 0.11). (**Figure 3.5**)

4. Discussion

Within an attention training closed-loop brain-computer interface, we observe a differential group effect of neurofeedback on EEG microstates. Specifically, microstate C had increased temporal presence in Non-Learners—those who were unsuccessful in self-regulating neural performance. Additionally, microstate D had increased temporal presence in Learners—those who were successful in self-regulating neural performance. Notably, however, this difference is apparent only over the entire training period and does not have a significant effect with training time. Thus, this provides evidence for the hypothesis that there are group differences in microstates within attention training, yet rejects the hypothesis that this difference is modulated by time.

We also find that microstate C, while significantly less present in Learners, also displays a positive relationship with efficiency specific to this group—that is, with greater microstate C presence in Learners, the better their efficiency. Furthermore, a similar but opposite trending relationship is observed in microstate D: while Learners overall display greater temporal presence of microstate D, that presence has a negative relationship with efficiency specific to that group.

On its face, these results appear self-contradictory, but this may instead indicate a complex interdependence between microstates. Here we observe temporal presence in only two microstates isolated from all other states, yet six microstates were derived, and they all have their own temporal characteristics. These states are inherently interdependent because time is inherently limited—for some microstates to have greater temporal presence, others must experience paucity.

Therefore, this constraint makes it relevant to investigate the relative proportion of microstate C to microstate D. In this analysis, Learners and Non-Learners again had marked differences in microstate proportionality. Namely, the Learners had a much more balanced temporal presence between the two microstates in comparison to Non-Learners, where their microstate C was more temporally dominant. Sham participants appeared to be a sort of middle ground between the Learners and Non-Learners, although they were only significantly different from the Non-Learners in this regard. It may be this balance that facilitates learning in this group rather than simply the amount of one state between groups. This analysis emphasizes the importance of analyzing microstates in context of other microstates, and that it is likely the microstate's complex interdependencies that emerge into meaningful changes in cognition.

In past microstate investigations, this interdependency has been accounted for using a metric known as transition probability. Transition probability attempts to quantify the probability that any state will transition into any other state under the assumption that all states follow a Markov process and that a high transition probability between two states is indicative of a high interdependent state association. However, recent literature has found that microstates unreliably follow such a Markov process (von Wegner, Tagliazucchi, & Laufs, 2017), thus throwing doubt upon Markov-chain modeled transition probability as an effective measure for microstate interdependence. Thus, here we use a proportionality instead.

It is also noteworthy to address that the neural feedback measured in this BCI task was an unrelated measure—frontal-visual alpha coherence—and not the focus of this analysis— microstates. Furthermore, microstate statistics were measured as an average over the entire session, and not recorded trial-by-trial as was coherence. Past investigations have found

microstates to be plastic in a BCI paradigm (Hernandez et al., 2016), yet this experiment was not designed for their specific observation, and thus is limited in describing the effect of training.

The overall data quality in these groups was also a limitation. Many participant's data had to be excluded from the analysis due to noisy data. Combined with the post-hoc regrouping, this may have negatively impacted the potential power of our results. The gender divide was also heavily sided toward women, adding another factor that may make these results less generalizable to a larger population. We believe that these factors were not substantial enough to significantly influence the findings, but they are considerations all the same.

Therefore, these results may instead be descriptive of a characterization between the different BCI groups—those who can self-regulate, those who can't self-regulate, and those given sham feedback. It appears that receiving feedback while effectively self-regulating attention indeed demands activation in attention-oriented brain connectivity as measured through microstate D. Similarly, it appears that inability to self-regulate despite genuine feedback involves a higher activation in brain connectivity associated with microstate C. It may also be telling that the Learners are the only group whose microstate dwell time relates significantly to performance. Future investigations should consider investigating the nuances in the underlying connectivity differences in BCI Learners vs Non-Learners.

Much of the microstate literature offers commentary on microstates as if their functional significance is uniform across people. The present investigation offers evidence to the contrary: suggesting functional significance underlying a microstate may have inherent variance in the population. Future research should also focus on unpacking this variability to contextualize the literature on microstate functional significance.

5. Conclusion

This analysis successfully highlights group differences in BCI performance. Namely, that Learners have higher temporal presence in microstate D compared to Non-Learners, and that Non-Learners have higher temporal presence in microstate C compared to Learners and Sham controls. It was notably not true that Learners had overall more microstate D than microstate C— in fact, they were the group where the two microstates were most temporally balanced. This balance between temporal measures in microstates may indicate a key difference between Learners and Non-Learners and warrants further research. This analysis failed to find meaningful changes over the training course, so future work should also consider more investigations into microstate plasticity with training, especially using training that specifically uses microstates as its index for successful self-regulation.

6. References

Anguera, J. A., Boccanfuso, J., Rintoul, J. L., Al-Hashimi, O., Faraji, F., Janowich, J., ... & Gazzaley, A. (2013). Video game training enhances cognitive control in older adults. Nature, 501(7465), 97.

Bigdely-Shamlo, N., Mullen, T., Kothe, C., Su, K. M., & Robbins, K. A. (2015). The PREP pipeline: standardized preprocessing for large-scale EEG analysis. Frontiers in neuroinformatics, 9, 16.

Bréchet, L., Brunet, D., Birot, G., Gruetter, R., Michel, C. M., & Jorge, J. (2019). Capturing the spatiotemporal dynamics of self-generated, task-initiated thoughts with EEG and fMRI. NeuroImage.

Britz, J., Van De Ville, D., & Michel, C. M. (2010). BOLD correlates of EEG topography reveal rapid resting-state network dynamics. Neuroimage, 52(4), 1162-1170.

Curran, E. A., & Stokes, M. J. (2003). Learning to control brain activity: A review of the production and control of EEG components for driving brain–computer interface (BCI) systems. Brain and cognition, 51(3), 326-336.

Delorme, A., & Makeig, S. (2004). EEGLAB: an open source toolbox for analysis of single-trial EEG dynamics including independent component analysis. Journal of neuroscience methods, 134(1), 9-21.

Hernandez, L. D., Rieger, K., Baenninger, A., Brandeis, D., & Koenig, T. (2016). Towards using microstate-neurofeedback for the treatment of psychotic symptoms in schizophrenia. A feasibility study in healthy participants. Brain topography, 29(2), 308-321.

Khanna, A., Pascual-Leone, A., & Farzan, F. (2014). Reliability of resting-state microstate features in electroencephalography. PLoS One, 9(12), e114163.

Michel, C. M., & Koenig, T. (2018). EEG microstates as a tool for studying the temporal dynamics of whole-brain neuronal networks: a review. Neuroimage, 180, 577-593.

Milz, P., Faber, P. L., Lehmann, D., Koenig, T., Kochi, K., & Pascual-Marqui, R. D. (2016). The functional significance of EEG microstates—associations with modalities of thinking. Neuroimage, 125, 643-656.

Morris, D. J., Tøndering, J., & Lindgren, M. (2019). Electrophysiological and behavioral measures of some speech contrasts in varied attention and noise. Hearing research, 373, 1-9.
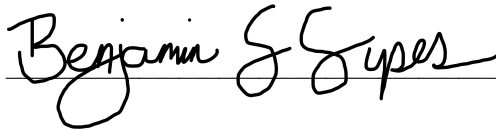
Pascual-Marqui, R. D., Lehmann, D., Faber, P., Milz, P., Kochi, K., Yoshimura, M., ... & Kinoshita, T. (2014). The resting microstate networks (RMN): cortical distributions, dynamics, and frequency specific information flow. arXiv preprint arXiv:1411.1949.

Pedroni, A., Bahreini, A., & Langer, N. (2018). AUTOMAGIC: Standardized Preprocessing of Big EEG Data. bioRxiv, 460469.

Poulsen, A. T., Pedroni, A., Langer, N., & Hansen, L. K. (2018). Microstate EEGlab toolbox: An introductory guide. bioRxiv, 289850.

Seitzman, B. A., Abell, M., Bartley, S. C., Erickson, M. A., Bolbecker, A. R., & Hetrick, W. P. (2017). Cognitive manipulation of brain electric microstates. Neuroimage, 146, 533-543.

Van de Ville, D., Britz, J., & Michel, C. M. (2010). EEG microstate sequences in healthy humans at rest reveal scale-free dynamics. Proceedings of the National Academy of Sciences, 107(42), 18179-18184.

von Wegner, F., Tagliazucchi, E., & Laufs, H. (2017). Information-theoretical analysis of resting state EEG microstate sequences-non-Markovianity, non-stationarity and periodicities. Neuroimage, 158, 99-111.

Wackermann, J., Lehmann, D., Michel, C. M., & Strik, W. K. (1993). Adaptive segmentation of spontaneous EEG map series into spatially defined microstates. International Journal of Psychophysiology, 14(3), 269-283.

Winkler, I., Haufe, S., & Tangermann, M. (2011). Automatic classification of artifactual ICA-components for artifact removal in EEG signals. Behavioral and Brain Functions, 7(1), 30.

Publishing Agreement

It is the policy of the University to encourage the distribution of all theses, dissertations, and manuscripts. Copies of all UCSF theses, dissertations, and manuscripts will be routed to the library via the Graduate Division. The library will make all theses, dissertations, and manuscripts accessible to the public and will preserve these to the best of their abilities, in perpetuity.

Please sign the following statement:

I hereby grant permission to the Graduate Division of the University of California, San Francisco to release copies of my thesis, dissertation, or manuscript to the Campus Library to provide access and preservation, in whole or in part, in perpetuity.

Benjamin S Sypes   9/6/2019

Author Signature   Date